Effect of water/glycerol polymorphism on dynamic nuclear polarization

Alisa Leavesley[1], C. Blake Wilson[2], Mark Sherwin,[2] Songi Han[1]

[1]Department of Chemistry and Biochemistry, University of California, Santa Barbara, Santa Barbara, CA

[2]Department of Physics, University of California, Santa Barbara, Santa Barbara, CA

Electronic Supplemental Information

1. Experimental Section

1.1. Sample preparation: 4-amino TEMPO (Sigma-Aldrich), deuterium oxide (Cambridge Isotopes), and d_8-glycerol (Cambridge Isotopes) were used as received. Solid red-orange crystals of 4AT radical were dissolved in a stock solution of 5:4:1 or 6:3:1 by volume of d_8-glycerol : D_2O : H_2O and diluted to 40 mM 4AT. Water was purified with a μ-Pure water system (Pure Power, Korea; 12.5 MΩ) prior to use. 40 μL of sample was pipetted into a cylindrical Teflon sample holder (7 mm o.d., 6 mm i.d., 7mm height) for use with our home-built 300 MHz NMR probe with a ^{1}H alderman grant inductively coupled coil. The sample cup and probe were cooled to 4 K by continuous helium flow in our custom-designed Janis STVP-NMR wide-bore cryostat.

1.2. Cooling rates: Two cooling rates were used in this study to reach 4 K as depicted in the main text (Fig. 1). Thermally controlled (TC) involved cooling at a rate of 1 K/min to a temperature 10 ($\pm$ 1) K above the T_g. The sample was then held at this temperature for 1 hour followed by cooling at 1 K/min to 100 K, then the cooling rate was increased to 12 K/min until 4 K was reached. In the second cooling method, fast cool (FC), the sample was cooled at a constant rate of 10 K/min from 290 K to 4 K. It should be noted that in both the FC and TC scenarios the actual cooling rates were dramatically reduced between 12 and 4 K due to thermal equilibrium as the boiling point of helium is approached – here the helium pressure to achieve the respective cooling rates was held constant even though the actual rate of cooling between 12 and 4 K was dramatically reduced.

1.3. 7 T dual DNP/EPR: The hardware for this instrument has been previously described.[1] The MW are produced from a frequency tunable YIG oscillating solid state source (Mircolambda) at 12 GHz with a 10 GHz bandwidth. The MW are then multiplied and amplified to 200 GHz and 140 μw (VDI) and are directed to the sample located in the sweet spot of our 7 T superconducting magnet (Bruker Biospin) with minimal power loss via a quasi-optical bridge and a corrugated waveguide (Thomas Keating Ltd.) inside of the magnet. At the end of the waveguide, the sample sits on top of a silver plated mirror, in our home-built NMR probe, which consists of an inductively-coupled Alderman-Grant ^{1}H coil.[2] The purpose of the mirror is to reflect the MWs back through the sample to increase the B_1. Induction mode EPR detection via a super-heterodyne detection scheme with an intermediate frequency of 3 GHz as describe in our previous publication was utilized.[1] A protect switch is used to remove residual electronic noise from the intermediate frequency stage due to the relatively high powered MW pulses compared to the EPR signal from the sample. Phase cycling (0 and 180°) was implemented by using an 11.25° phase shifter at 12 GHz before the frequency and phase are multiplied x16 to 200 GHz and 180°. The probe and waveguide are placed inside of our custom Janis STVP-NMR continuous flow cryostat that can be operated at

temperatures >3 K. Automated control of the MW for DNP and EPR were achieved with Specman4EPR. All DNP and NMR experiments were conducted at 7 T and at 4 K, using a Bruker 300 Avance solid-state NMR spectrometer. A saturation recovery pulse sequence followed by a 60 s delay under MW irradiation with solid echo detection (90x-t-90y) with an inter-pulse delay, t = 130 μs, was used to measure the recovered ^{1}H magnetization under DNP for all experiments. Solid state-DNP profiles were obtained by measuring the NMR signal enhancement as a function of MW irradiation frequency using the full MW power (~120 μw). The signal enhancement, ε_{60}, is quantified by the ratio of the area of the NMR signal with MW on after 60 s of irradiation ($S_{on,60}$) relative to the area of the NMR signal with MW off at equilibrium ($S_{off,eq}$), ie ($\varepsilon_{60}=S_{on,60}/S_{off,eq}$). The ε_{60} was adjusted to represent steady state by extrapolating $S_{off,eq}$ to their equilibrium values according to $M_Z(t) = M_{eq}\left[1 - exp\left(-{}^{t}/_{T_x}\right)\right]$, where T_x is T_{1n} (spin-lattice relaxation, for MW off). T_{1n} was taken from a previous publication for a 541 FC sample and was assumed to be the same for all of the samples in this study [3]. Phase memory time (T_m) measurements are a standard EPR experiment, two short pulses (500 ns) to produce a Hahn echo that was digitized to Specman4EPR, the time delay between the echo forming pulses are incremented to determine T_m when fit to a bi-exponential. The interpulse delay between the echo forming pulses was incremented from 400 ns - 16 μs.

1.4. 8.5 T EPR

EPR measurements at 240 GHz were carried out on a home-built spectrometer operating with an Oxford instruments magnet with a sweep range of 0-12.5 T.[4] Measurements were conducted at 8.56 T using a 55 μw Virginia Diodes, Inc, microwave source, and induction-mode, super-heterodyne detection was employed. Lineshapes were obtained using cw- and pulsed techniques. CW lineshapes were acquired using 3-6 μW of incident power, with 20 kHz, 5 Gauss peak-to-peak field modulation. Lineshapes were also obtained using field-swept echo experiments, consisting of two 55 μW, 1 μs long pulses with an inter-pulse delay of 3 μs to generate an echo, whose amplitude was recorded as a function of field. T_m measurements were carried out using two 55 μW, 1 μs long pulses. Phase cycling was not employed, and as a consequence the minimum inter-pulse delay was limited to ~2.5 μs, and incremented to 22 μs. Echo decay curves were well described by a stretched exponential $V(2\tau) = exp\left(-\left({}^{2\tau}/_{\tau_m}\right)^{x}\right)$ with x = 3/2.The reported T_m values are the average decay times, $T_m = \Gamma\left(1 + {}^{1}/_{x}\right)\tau_m \approx 0.90\tau_m$ [5]

1.5. DSC

A TA Instruments Q2000 DSC with 50 position autosampler, sensitivity < 0.2 μW, and baseline drift < 10 μW was used to collect the heating and cooling curves for the different samples and freezing methods. An Indium-sapphire standard was used for calibration of the heat capacity. Samples underwent three heating and cooling cycles. The cooling cycles were cooled with liquid nitrogen down to 103 K as described in section 1.2, during the

heating cycles, the samples were heated at a rate of 10 K/min to 300 K for both cooling methods. The T_g was extracted from the second heating cycle.

2. cw-EPR lineshape simulation

The EPR lineshapes as described in the main text show the overall electron environment. The general EPR lineshapes are practically identical for both of the 631 freezing conditions (main text) and is similar for 541-FC. The cw-EPR spectra appear to have two populations of g_{xx}. Thus, the cw-EPR spectra were simulated to determine the relative populations for these two components with EasySpin, a MATLAB EPR simulation tool. All of the y- and z- components and most of the x-components between the two species were set to be the same (All parameters are provided in SITable 1). The g_{xx} of one species was set to 2.00787, while the other had a g_{xx} of 2.00837, which results in a 250 ppm separation between the two species' g_{xx}'s. The weighting between the two components were then varied to simulate the experimental spectra presented here. A comparison of the simulations to the experimental spectra are shown in SIfigure 1, while the relative populations of the two species are reported in SITable 1. The simulations are reasonable considering only the ratio between the two species is changed and that all strains are substantially lower than their respective values. We find that all of the spectra contain both species, while the 631 samples and 541-FC are weighted similarly, where the high field species is favored. The 541-TC sample instead favors the low field species. Since the separation between the g_{xx} of the two species is 250 ppm, which could roughly correspond to a shift in the hydrogen bonding network to the nitroxide moiety by one – 205 ppm (g_{xx1} = 2.00831 for one H-bond and g_{xx2} = 2.00831 for two H-bonds),[6] then the 541-TC system could be said to favor a low hydrogen bonding environment compared to the other three systems.[7] It is interesting to note that between the two freezing methods, the TC freezing method does have a higher ratio for the low field species independent of solvent. However, the 631 solvent is not as affected as the 541 solvent, indicating that the 631 solvent resists variations in its polymorphs, unlike 541. The higher ratio of the low field species with TC freezing method supports the DNP results that indicate radical clustering. These combined results suggest that in general the 631-TC, 631-FC, and 541-FC have similar overall electron spin environments and thus should have more similar radical distributions in the glassy matrices, whereas 541-TC has a different overall radical heterogeneity.

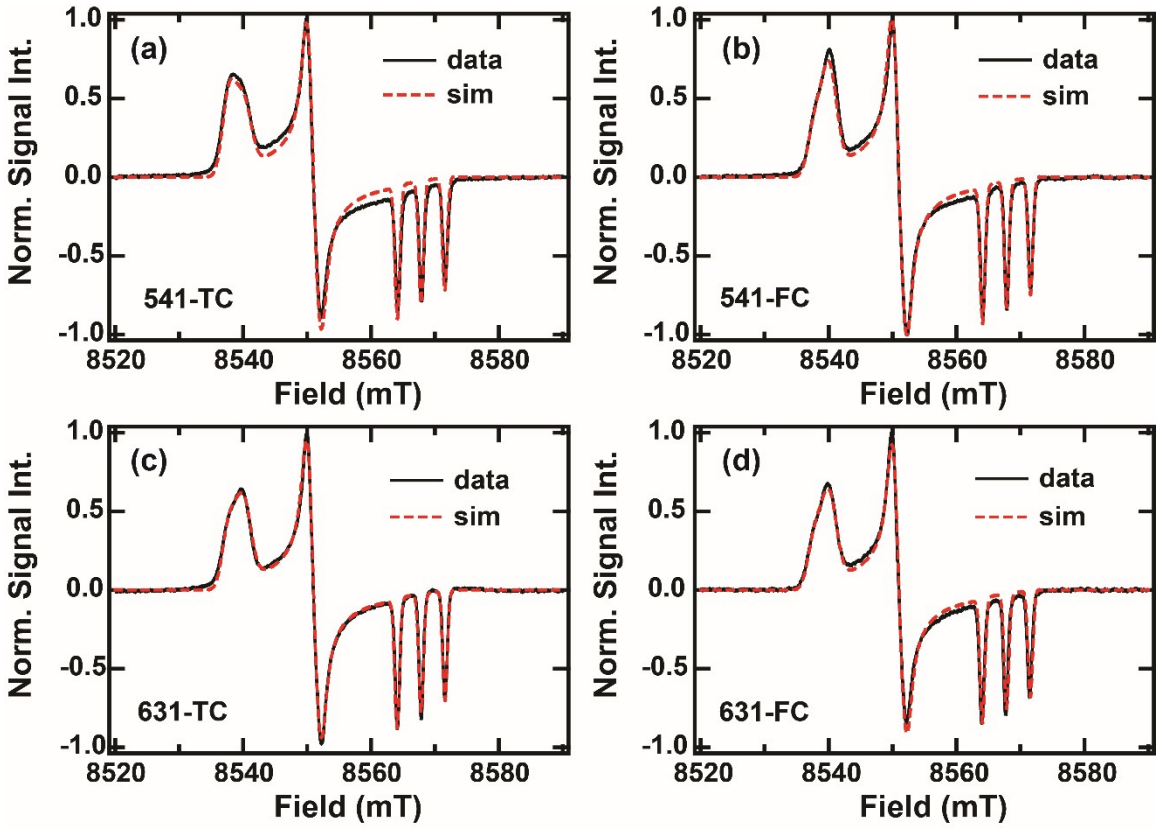

SIFigure 1. *Simulated cw-EPR spectra (red-dashed) of 40 mM 4-amino TEMPO for the four systems are compared to the experimental spectra (black-solid) at 8.5 T. The weighting of the two components for the simulations are shown in SITable 1 with the other simulation parameters.*

.

SITable 1. *Relative populations of the two components for the simulated cw-EPR spectra for each of the four systems. Parameters for EasySpin simulations are the following: S=1/2, nucleus = ^{14}N, g_{yy} = 2.00527, g_{zz} = 2.001375, A = [18 18 105], gStrain = [0.00032 0 0], Astrain = [4 0 0], HStrain = [40 40 20], lw = 0.5, mwFreq = 240 GHz, temperature = 4.5 K, and method = matrix.*

Sample	% of population	
	Low field (g_{xx}=2.00839)	High field (g_{xx}=2.00787)
541-TC	55	44
541-FC	33	67
631-TC	44	56
631-FC	37	63

3. Comparison of T_m at 7 T and 8.56 T

It should be noted that the T_m values measured at 7 T are less consistent across the EPR line since the experimental data was fitted with a bi-exponential curve to extract the T_m time constant compared to a stretched exponential fit for the T_m measurements taken at 8.56 T. The reason for the different fits at the two magnetic fields is due to the different dead times for the two spectrometers, where the dead time at 7 T is ~ 300 ns due to incorporation of phase cycling, while the dead time at 8.56 T is ~2 μs without phase cycling. However, despite

the differences in these home-built spectrometers, the overall trends at both magnetic fields are the same, which allows EPR results taken at 8.56 T to be compared with the DNP results at 7 T.

The echo decay curves that were used to extract T_m are shown in SIfigure 2 for both magnetic fields. The fit for each echo decay is shown as a dashed line, where the 7 T data was fit to $y = Aexp^{-2t/T_{m1}} + Bexp^{-2t/T_{m2}} + C$, where C is a constant, T_{m2} is very short (<500 ns) and T_{m1} is reported in the main text as T_m. The 8.56 T data was fit to a stretched exponential of the form $y = Aexp\left(-\left(2t/T\right)^x\right) + C$, where C is a constant, $x = 3/2$, and the T_m reported in the main text is the average decay rate, given by $T_m = \Gamma\left(1 + 1/x\right)T \approx 0.90T_{.5}$

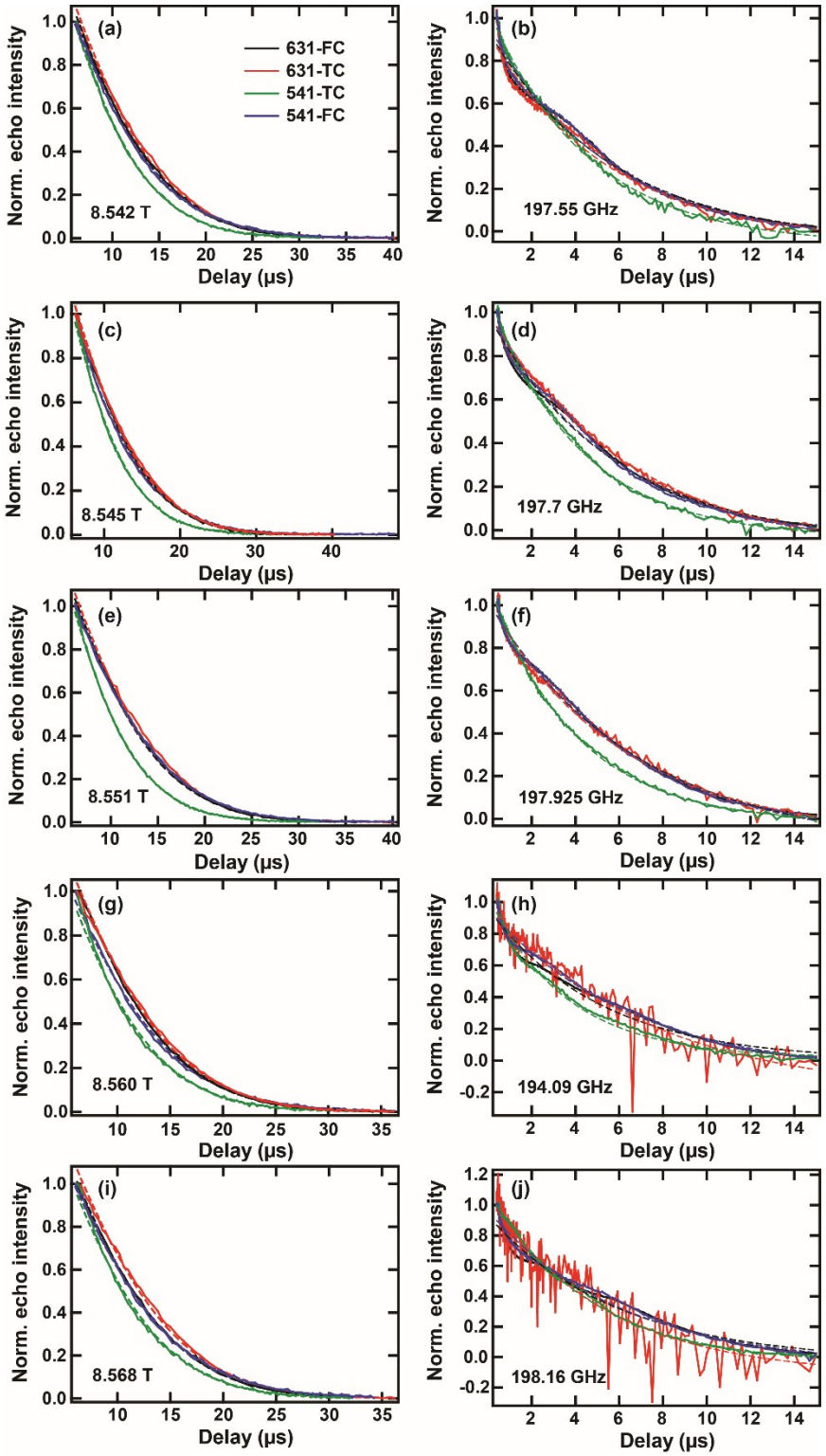

SIFigure 2. *Echo decay curves for 40 mM 4-amino TEMPO in 5:4:1 and 6:3:1 d_8-glycerol:D_2O:H_2O when cooled via TC and FC at five positions across the EPR line at 8.56 T (a,c,e,g,i) and 7 T (b,d,f,h,j). At 8.56 T, the frequency of MW irradiation was held constant at 240 GHz and the field was changed, while the corresponding 7 T data is acquired by changing the frequency. Experimental parameters for 8.56 T are t_p = 1000 ns and repetition time = 240 ms, while at 7 T they are t_p = 500 ns and repetition time = 500 ms.*

4. Dynamic nuclear polarization

DNP is a process where electron polarization is transferred to surrounding nuclei via two common mechanisms: the solid effect (SE)[8,9] and the cross effect (CE).[8,10–12] The SE DNP mechanism involves irradiating microwaves (MW) on the forbidden transitions: zero quantum (ZQ) and double quantum (DQ), between a single electron and its hyperfine coupled nuclei. The SE occurs when radicals are sufficiently separated that they are unable to dipolar couple to each other. The SE results in the peak-to-peak (positive to negative) frequency difference (Δ_{DNP}) to be equal to $2\omega_0$ - here 600 MHz, and allows for DNP enhancement outside of an EPR spectrum that consists solely of allowed EPR transitions. The CE DNP mechanism is the transfer of polarization between two or more dipolar coupled electrons to their surrounding nuclei. The CE effect occurs when the frequency difference between the dipolar coupled electrons is equal to the Larmor frequency of the hyperfine coupled nuclei, aka the CE condition. When the CE condition is met, then the polarization difference between the electrons spins due to MW irradiation is transferred to the surrounding hyperfine coupled nuclei, causing nuclear signal enhancement and results in all DNP enhancement occurring within the EPR spectrum consisting solely of allowed transitions and $\Delta_{DNP} < 2\omega_0$.

Selected DNP spectra of the four systems of 40 mM 4-amino TEMPO studied here are shown in SIfigure 2, while multiple-day average DNP spectra are shown in the main text. The spectra are taken at different applied MW powers in order to obtain the maximum positive DNP enhancement for each system. All four spectra have identical Δ_{DNP}'s of 400 MHz that is less than $2\omega_0$, which when combined with the fact that the whole DNP spectra falls within the allowed transition EPR line is indicative of the CE-DNP mechanism. From these selected spectra, we can see that the 631 spectra are essentially identical independent of the freezing condition. The 541 system shows that the span of the DNP spectra at 50% of the signal enhancement is dependent on the freezing condition. Interestingly, the 541-FC has effectively the same span at 50% signal enhancement compared to the 631 systems. This supports the previously described data, where 541-TC forms a different glass and has a different radical distribution.

When considering the lower concentration DNP profiles of 5 mM, both the CE and SE DNP mechanisms are observed in the profile lineshapes (The 5 mM DNP profile is shown again here for convenience in SIFig. 2c). The Δ_{DNP} of the TC sample is 400 MHz, while that of FC is 450 MHz. Combined with the fact that more DNP enhancement falls outside of the width of the allowed EPR spectrum for FC suggests that the FC system is governed more heavily by the SE DNP mechanism, while the narrower DNP spectra for TC implies a slightly more prevalent CE DNP mechanism. The implication of a more CE dominated TC sample is that the local radical concentration is higher in the TC sample than the FC sample. To further illustrate this analysis, SIfigure 3 directly compares the DNP spectra of the 5 mM 4AT samples with that of 40 mM 4AT 541-FC. Here we see that neither of the 5 mM spectra are solely influenced by the CE DNP mechanism as the span of the 40 mM spectra is significantly narrower at 50% of the normalized signal; however, the span of the TC sample's DNP spectrum is

slightly narrower at 50% of the normalized signal and has exactly the same Δ_{DNP} as the 40 mM sample, which suggests a larger CE mechanistic contribution for TC compared to FC.

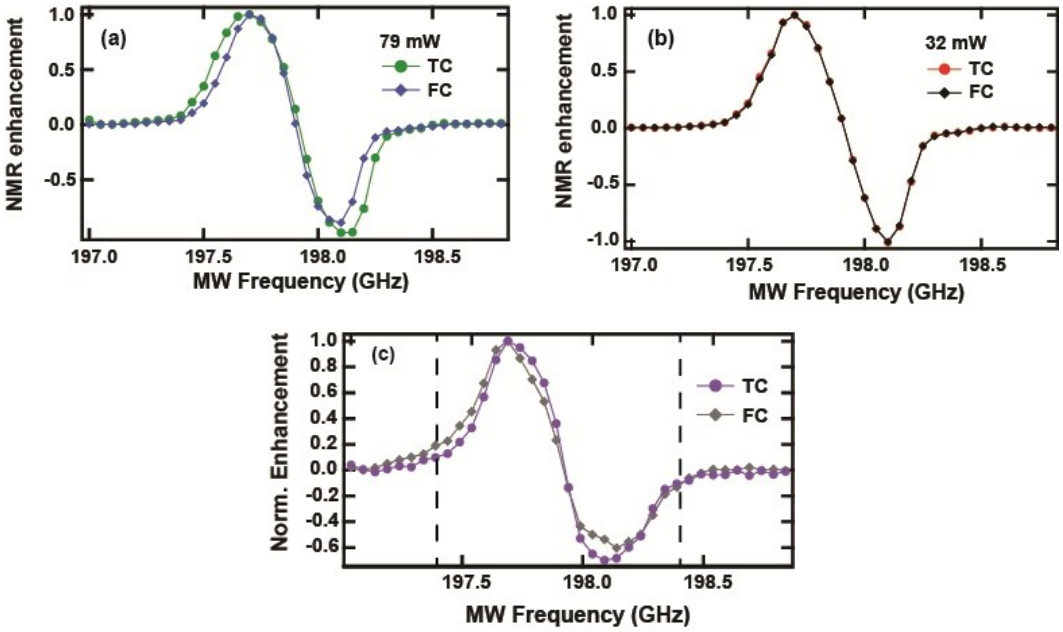

SIFigure 3. *DNP profiles comparing the freezing conditions (FC and TC) of 40 mM 4AT in 5:4:1 (a), 6:3:1 (b), and 5 mM 4AT in 5:4:1 (c) d_8-gylcerol:D_2O:H_2O taken at 7 T and 4K. The dashed vertical lines in (c) represent the width of the allowed EPR spectrum. (c) was acquired at 6.91 T and the frequency in (c) was scaled by 4 GHz to represent data acquired at 7 T for comparison to the rest of the data presented here. All spectra were normalized to the maximum signal intensity. Lines are drawn to guide the eye.*

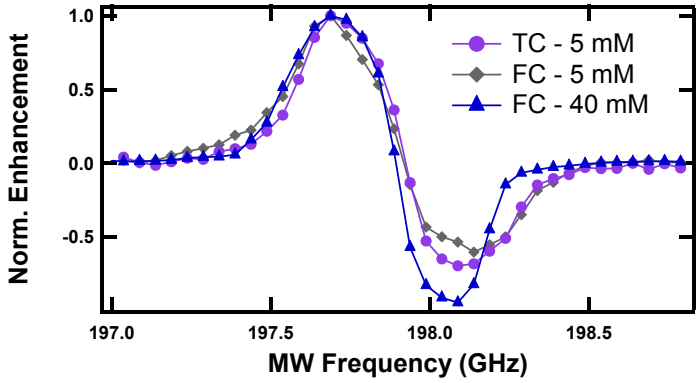

SIFigure 4. *DNP profiles comparing the freezing conditions (FC and TC) of 5 mM 4AT and 40 mM FC in 5:4:1 d_8-gylcerol:D_2O:H_2O taken at 7 T and 4K. The 5 mM spectra were acquired at 6.91 T and the frequency was scaled by 4 GHz to represent data acquired at 7 T for comparison to the rest of the data presented here. All spectra were normalized to the maximum signal intensity. Lines are drawn to guide the eye*

References:

1 T. A. Siaw, A. Leavesley, A. Lund, I. Kaminker and S. Han, *J. Magn. Reson.*, 2016, **264**, 131–153.

2 T. A. Siaw, S. a. Walker, B. D. Armstrong and S.-I. Han, *J. Magn. Reson.*, 2012, **221**, 5–10.

3 T. a. Siaw, M. Fehr, a. Lund, a. Latimer, S. a. Walker, D. T. Edwards and S. Han, *Phys. chem. chem. phys.*, 2014, **16**, 18694–18706.

4 S. Takahashi, L. C. Brunel, D. T. Edwards, J. van Tol, G. Ramian, S. Han and M. S. Sherwin, *Nature*, 2012, **489**, 409–413.

5 M. N. Berberan-Santos, E. N. Bodunov and B. Valeur, *Chem. Phys.*, 2005, **315**, 171–182.

6 E. Bordignon, A. I. Nalepa, A. Savitsky, L. Braun and G. Jeschke, *J. Physcial Chem. B*, 2015, **119**, 13797–13806.

7 E. Bordignon, H. Brutlach, L. Urban, K. Hideg, A. Savitsky, A. Schnegg, P. Gast, M. Engelhard, E. J. J. Groenen, K. Möbius and H. J. Steinhoff, *Appl. Magn. Reson.*, 2010, **37**, 391–403.

8 C. T. Farrar, D. a. Hall, G. J. Gerfen, S. J. Inati and R. G. Griffin, *J. Chem. Phys.*, 2001, **114**, 4922–4933.

9 Y. Hovav, A. Feintuch and S. Vega, *J. Magn. Reson.*, 2010, **207**, 176–189.

10 Y. Hovav, O. Levinkron, A. Feintuch and S. Vega, *Appl. Magn. Reson.*, 2012, **43**, 21–41.

11 D. Shimon, Y. Hovav, A. Feintuch, D. Goldfarb and S. Vega, *Phys. Chem. Chem. Phys.*, 2012, **14**, 5729–5743.

12 Y. Hovav, A. Feintuch and S. Vega, *J. Magn. Reson.*, 2012, **214**, 29–41.